

Supporting information for

Trimetallic CoFeCr hydroxide electrocatalysts synthesized at low temperature for accelerating water oxidation via tuning electronic structure of active sites

Yibin Yang,^a Xun Cui,^b Di Gao,^c Huichao He,^d Yingqing Ou,^c Ming Zhou,^c Qingxin Lai,^c Xijun Wei,^c Peng Xiao^{a,*} and Yunhuai Zhang^{c,*}

^a Chongqing Key Laboratory of Soft Condensed Matter Physics and Smart Materials, College of Physics, Chongqing University, Chongqing 400030, China.

^b Key Laboratory of Catalysis and Energy Materials Chemistry of Ministry of Education & Hubei Key Laboratory of Catalysis and Materials Science, South-Central University for Nationalities, Wuhan 430074, China

^c College of Chemistry and Chemical Engineering, Chongqing University, Chongqing 400030, China

^d State Key Laboratory of Environmental-Friendly Energy Materials, School of Materials Science and Engineering, Southwest University of Science and Technology, Mianyang 621010, China

Corresponding Author

Name: Peng Xiao (xiaopeng@cqu.edu.cn); Yunhuai Zhang (xp2031@163.com)

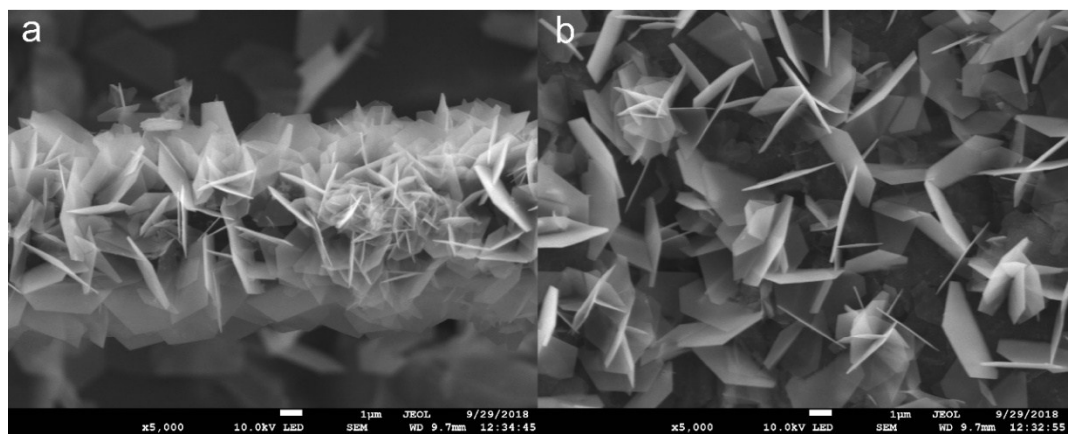


Figure S1 a) and b) SEM images of CoFeCr-6:2:1 with different magnification.

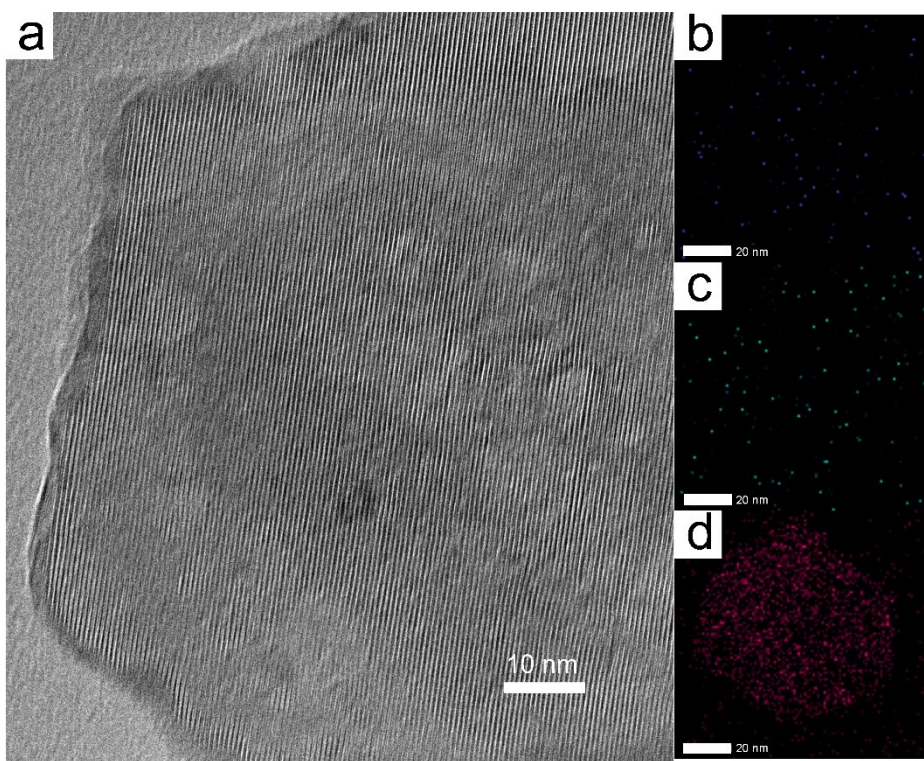


Figure S2 a) HRTEM image of CoFe-2:1; b), c), and d) Element mapping of Co, Fe and O, respectively.

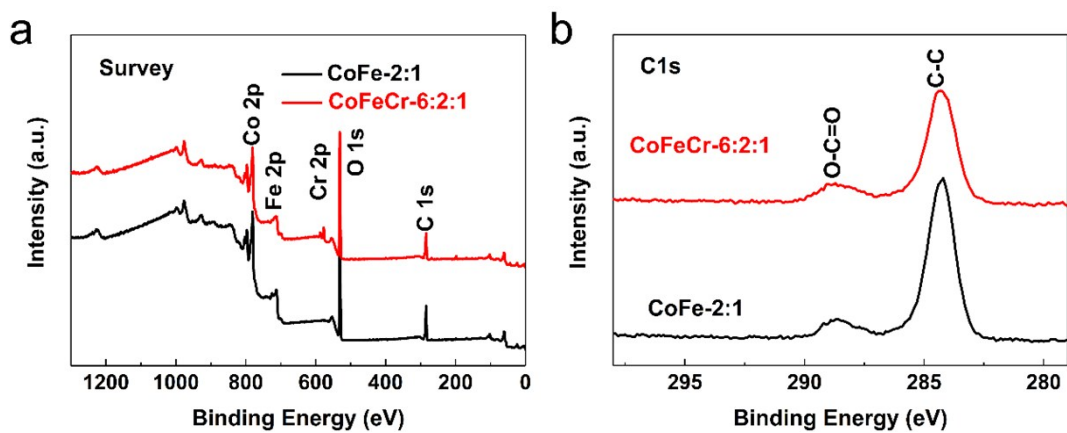


Figure S3 a) XPS survey of CoFe-2:1 and CoFeCr-6:2:1, b) High-resolution XPS spectra of C 1s spectrum of CoFe-2:1 and CoFeCr-6:2:1.

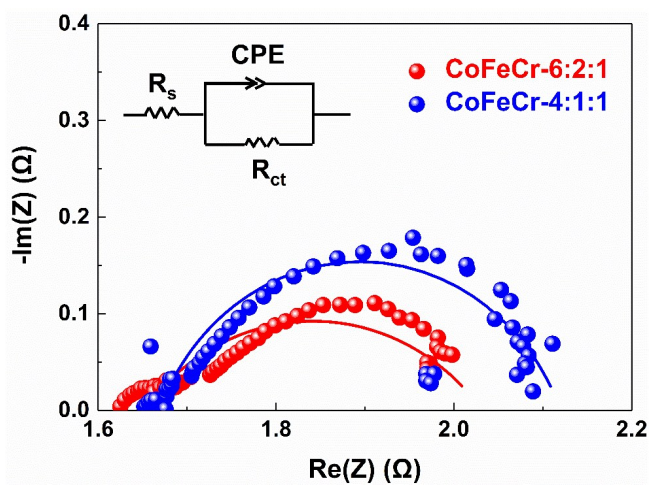


Figure S4 The Nyquist plots of CoFeCr-6:2:1 and CoFeCr-4:1:1. Inset shows the corresponding equivalent circuit.

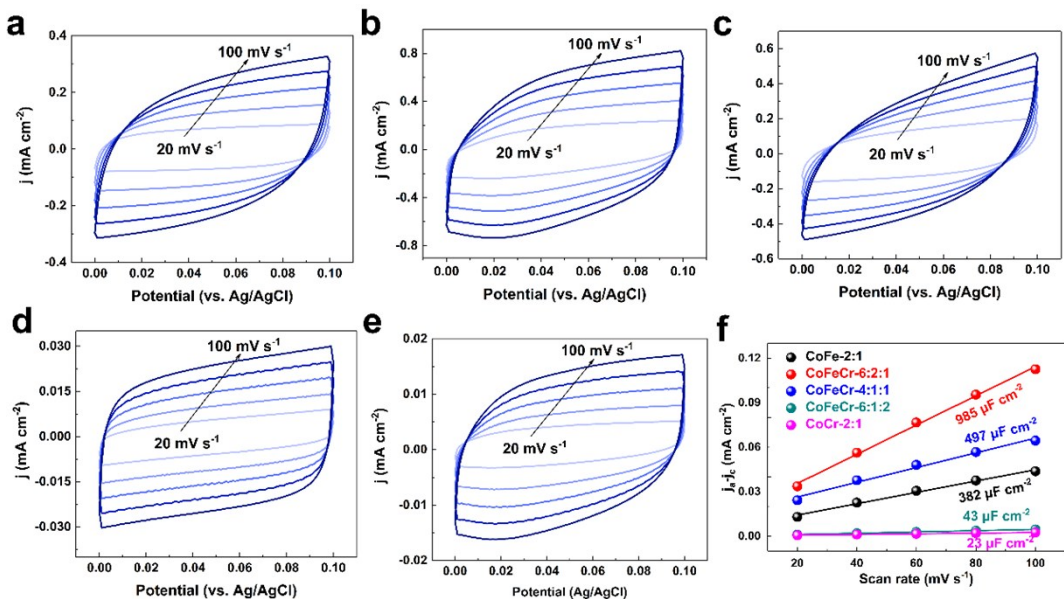


Figure S5 Electrochemical active surface area analysis. CVs of a) CoFe-2:1, b) CoFeCr-6:2:1, c) CoFeCr-4:1:1, d) CoFeCr-6:1:2, and e) CoCr-2:1 at different scan rates (20 mV s^{-1} , 40 mV s^{-1} , 60 mV s^{-1} , 80 mV s^{-1} , and 100 mV s^{-1}). f) Linear fitting of capacitive currents of the sample vs. scan rate.

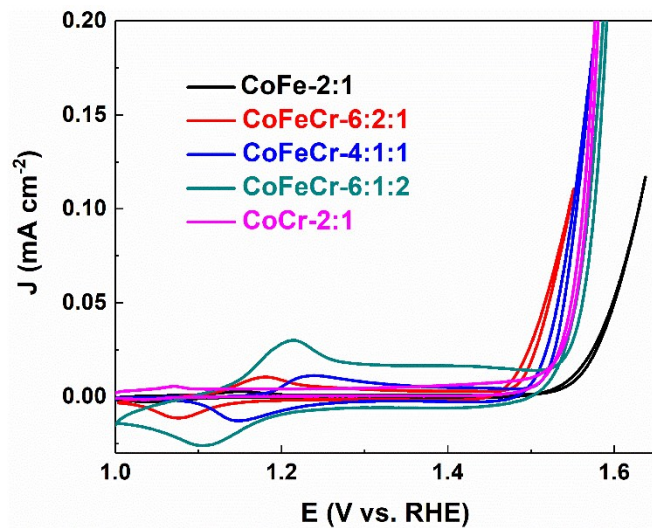


Figure S6 OER polarization curves normalized by ECSA

Table S1 Summary of the fitting parameters obtained from the Nyquist plots.

	Tafel slope		C _{dl}		EIS		
	R ²	R ²	R _s	R _{ct}	CPE-P	CPE-T	Chi-Squared
CoFe-2:1	0.989	0.998	1.83	1.864	0.75298	0.01992	0.0070495
CoFeCr-6:2:1	0.995	0.985	1.651	0.381	0.57349	0.32552	0.0030234
CoFeCr-4:1:1	0.969	0.994	1.668	0.452	0.75511	0.19904	0.0017365
CoFeCr-6:1:2	0.955	0.995	1.711	1.889	0.83177	0.019841	0.0012523
CoCr-2:1	0.959	0.999	1.659	2.397	0.89126	0.01071	0.0029008

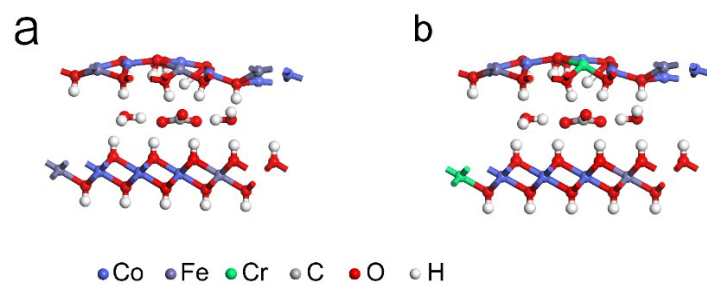


Figure S7 a) and b) Side views of the models of CoFe-2:1 and CoFeCr-6:2:1 for DFT calculations. The (001) surface are exposed for electrocatalytic OER.

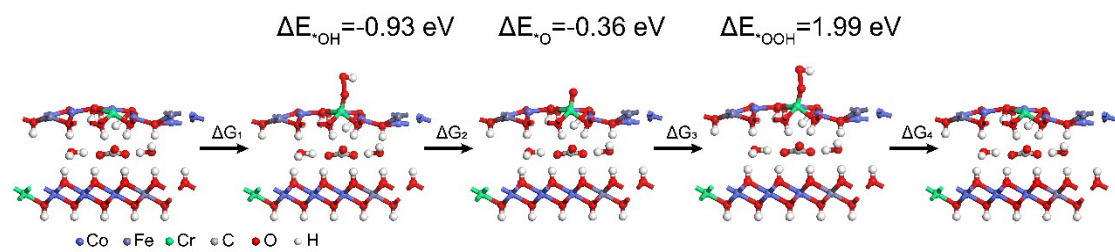


Figure S8 DFT theoretical models of CoFeCr-6:2:1. Structures and bond energies of *OH, *O, and *OOH intermediates adsorbed on the Cr sites of the model.

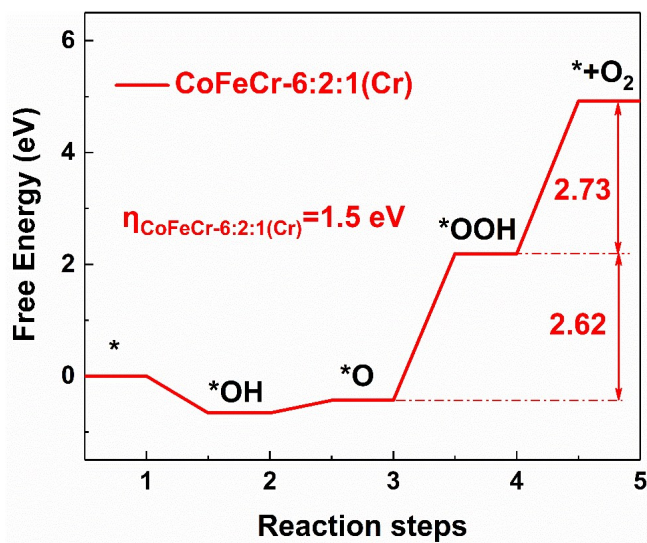


Figure S9 Calculated Gibbs free-energy diagram of OER on the Cr sites of CoFeCr-6:2:1.

Table S2 DFT results for metal 3d and O 2p band center in the samples.

sample	Co	Fe
Co ₂ Fe	2.64	2.67
Co ₂ Fe _{0.5} V _{0.5}	2.61	2.91

Table S3 Comparison of catalytic performance of CoFeCr-6:2:1 hydroxide to recently reported high performance metal oxide/hydroxide OER electrocatalysts.

Elecatalyst	electrolyte	j (mA cm ⁻²)	η (mV)	Tafel slope (mV dec ⁻¹)	Ref.
CoFeCr-6:2:1 LDH@CP	1.0 M KOH	10	260	40.1	This work
NiFe LDH-CoC/AB composite	6.0 M KOH	10	289	-	1
Fe-doped Co₃V₂O₈/GC	1.0 M KOH	10	307	36	2
CoMoO NSs@NF	1.0 M KOH	10	270	54.4	3
Fe-UTN/GC	1.0 M KOH	10	270	36.6	4
Porous CoO_x/GC	1.0 M KOH	10	306	67	5
CoFe-LDH/rGO	0.1 M KOH	10	325	-	6
Co₂P/CP	1.0 M KOH	10	310	61	7
Co Intercalated NiFe LDH	1.0 M KOH	10	265	47	8
R-CoPx/rGO(O)/GC	1.0 M KOH	10	268	66	9
Co–Fe Oxyphosphide	1.0 KOH	10	280	53	10
LiCoO_x/CP	0.1 M KOH	10	290	50	11
PA-CoS_x(OH)_y/NF	1.0 M KOH	10	261	-	12
ELCMO/GC	1.0 M KOH	10	329	33.8	13
Ni-BDC/Ni(OH)₂/GC	1.0 M KOH	10	320	41	14
DH-CoFe LDHs	1.0 M KOH	10	276	40.3	15

Reference :

1. Q. Wang, D. Zhou, H. Yu, Z. Zhang, X. Bao, F. Zhang and M. Zhou, *J. Electrochem. Soc.*, 2015, **162**, A2362-A2366.
2. T. Gao, Z. Jin, M. Liao, J. Xiao, H. Yuan and D. Xiao, *J. Mater. Chem. A*, 2015, **3**, 17763-17770.
3. Y. Zhang, Q. Shao, S. Long and X. Huang, *Nano Energy*, 2018, **45**, 448-455.
4. G. Shen, R. Zhang, L. Pan, F. Hou, Y. Zhao, Z. Shen, W. Mi, C. Shi, Q. Wang, X. Zhang and J.-J. Zou, *Angew. Chem. Int. Ed.*, 2019, DOI: 10.1002/anie.201913080.
5. W. Xu, F. Lyu, Y. Bai, A. Gao, J. Feng, Z. Cai and Y. Yin, *Nano Energy*, 2018, **43**, 110-116.
6. X. Han, C. Yu, J. Yang, C. Zhao, H. Huang, Z. Liu, P. M. Ajayan and J. Qiu, *Adv. Mater. Interfaces*, 2016, **3**, 1500782.
7. M. Song, Y. He, M. Zhang, X. Zheng, Y. Wang, J. Zhang, X. Han, C. Zhong, W. Hu and Y. Deng, *J. Power Sources*, 2018, **402**, 345-352.
8. A. C. Thenuwara, N. H. Attanayake, J. Yu, J. P. Perdew, E. J. Elzinga, Q. Yan and D. R. Strongin, *J. Phys. Chem. B*, 2018, **122**, 847-854.
9. X. Zhou, H. Gao, Y. Wang, Z. Liu, J. Lin and Y. Ding, *J. Mater. Chem. A*, 2018, **6**, 14939-14948.
10. P. Zhang, X. F. Lu, J. Nai, S. Q. Zang and X. W. D. Lou, *Adv. Sci.*, 2019, **6**, 1900576.
11. Z. Lu, H. Wang, D. Kong, K. Yan, P.-C. Hsu, G. Zheng, H. Yao, Z. Liang, X. Sun and Y. Cui, *Nat. Commun.*, 2014, **5**.
12. Y. Zeng, L. Chen, R. Chen, Y. Wang, C. Xie, T. Li, L. Huang and S. Wang, *J. Mater. Chem. A*, 2018, **6**, 24311-24316.
13. T. Maiyalagan, K. A. Jarvis, S. Therese, P. J. Ferreira and A. Manthiram, *Nat. Commun.*, 2014, **5**, 3949.
14. D. Zhu, J. Liu, L. Wang, Y. Du, Y. Zheng, K. Davey and S. Z. Qiao, *Nanoscale*, 2019, **11**, 3599-3605.
15. P. Zhou, J. He, Y. Zou, Y. Wang, C. Xie, R. Chen, S. Zang, S. Wang, *Sci. China Chem.*, 2019, **62**, 1365-1370.